Received: 17 March 2021 | Revised: 25 July 2021 | Accepted: 27 July 2021

DOI: 10.1111/adb.13086

ORIGINAL ARTICLE

Addiction Biology SSA WILEY

MicroRNA-132 is involved in morphine dependence via modifying the structural plasticity of the dentate gyrus neurons in rats

Meng Jia[1,2,3] | Xuewei Wang[1] | Haolin Zhang[1] | Xinjuan Wang[1] | Hui Ma[1] | Mingda Yang[1] | Yijing Li[1] | Cailian Cui[1]

[1]Department of Neurobiology, School of Basic Medical Sciences, Key Laboratory for Neuroscience of Ministry of Education and National Health Commission of China, Neuroscience Research Institute, Peking University, Beijing, China

[2]Beijing Tiantan Hospital, Capital Medical University, Beijing, China

[3]Center for basic and translational medicine, National Clinical Research Center for Neurological Disease, Beijing, China

Correspondence
Yijing Li and Cailian Cui, Department of Neurobiology, School of Basic Medical Sciences, Key Laboratory for Neuroscience of Ministry of Education and National Health Commission of China, Neuroscience Research Institute, Peking University, Beijing 100191, China.
Email: liyijing@bjmu.edu.cn; clcui@bjmu.edu.cn

Funding information
National Basic Research Development Program of China, Grant/Award Number: 2015CB553500; National Natural Science Foundation of China, Grant/Award Numbers: 81471353, 81771433; Natural Science Foundation of Beijing, Grant/Award Number: 7214224

Abstract

Repeated morphine exposure has been shown to induce neuronal plasticity in reward-related areas of the brain. miR-132, a CREB-induced and activation-dependent microRNA, has been suggested to be involved in the neuronal plasticity by increasing neuronal dendritic branches and spinogenesis. However, it is still unclear whether miR-132 is related to morphine dependence. Here, we investigate whether miR-132 is involved in morphine dependence and whether it is related to the structural plasticity of the dentate gyrus (DG) neurons. Sprague–Dawley rats are treated with increasing doses of morphine injection for six consecutive days to develop morphine dependence. Our results show that dendritic branching and spinogenesis of the DG neurons of morphine dependent rats are increased. Morphine treatment (24 h) promotes the differentiation of N2a cells stably expressing μ-opioid receptor by up-regulating miR-132 expression. Moreover, inhibiting miR-132 3p (but not 5p) of the DG neurons can reverse the structural plasticity and disrupt the formation of morphine dependence in rats. These findings indicate that miR-132 in the DG neurons is involved in morphine dependence via modifying the neuronal plasticity.

KEYWORDS
microRNA, morphine dependence, structural plasticity

1 | INTRODUCTION

Opioid use disorder (OUD) is a chronic relapsing disorder, and repeated opioid exposure will progress to opioid dependence, which is characterized by serious withdrawal symptoms and uncontrollable drug craving behaviour after morphine abstinence, which then leads to relapse.[1,2] Morphine, a widely used opioid analgesic in clinical practice, is the most common drug in OUD. Morphine dependence is widely believed to be the result of neuroadaptation and neuroplasticity caused by repeated morphine administration.[3,4] Neuronal plasticity is largely represented by restructuring of neurons in the reward-associated brain regions, which includes two types: changes in the size of cell bodies[5] and changes in dendritic arborizations or spine morphology.[6] Morphine exposure-induced structural plasticity is observed mostly in the mesolimbic dopamine system and other pathways mediating rewarding, among which the dentate gyrus (DG) of the hippocampus, a part of the limbic system, is long thought to mediate spatial memory[7] and context-associated memory of drug abuse.[8–10] Moreover, recent studies reveal that the DG is activated in morphine-dependent rodents.[11–15] Rats receiving 10 days successive increasing doses of morphine treatment display an evident c-fos induction in the DG.[15] Brain imaging research in rats shows that

Meng Jia and Xuewei Wang contributed equally.

repeated increasing doses of morphine treatment significantly enhance the blood-oxygen-level-dependent (BOLD) signal in the DG.[14] Thus, the DG may also be responsible for mediating morphine rewarding and dependence. However, to date, little is known about the neuronal plasticity in the DG of morphine-dependent rodents.

Additionally, the neuronal plasticity and behavioural abnormalities induced by morphine dependence can sustain for years or even decades, and such a process has been confirmed to be mediated by the gene expression regulatory mechanism.[16–20] Among numerous transcription factors, CREB (cAMP response element binding protein) is found to mediate the persistent changes induced by morphine dependence,[3,18] especially the changes in structural plasticity.[21] CREB binds to CRE (cAMP response element) and activates the expression of downstream genes, among which is miR-132, a neuronal plasticity-associated microRNA (miRNA).[22] miR-132 is an endogenous miRNA expressed in multiple organs and controls gene expression post-transcriptionally.[23] In the central nervous system, miR-132 is responsible for regulating neurogenesis and differentiation, including axonal sprouting and dendritic morphological plasticity.[23] miR-132 overexpression in hippocampal slices can significantly increase the total dendritic length of pyramidal neurons in the CA1, whereas miR-132 inhibition shows the opposite effect.[24] Meanwhile, miR-132 overexpression in vivo increases the dendritic spine density of pyramidal neurons in the CA1,[25] indicating that miR-132 is involved in modifying the structural plasticity of the hippocampal neurons. Interestingly, miR-132 also participates in morphine-induced neuronal adaptions. Our previous research showed that morphine treatment can induce miR-132 expression in neural stem cells (NSCs). Specific overexpression of miR-132 in the DG NSCs promotes the neuronal differentiation characterized by increases in the total dendritic length and spine density. It simultaneously mediates the formation of morphine addiction behaviours in rats.[9]

Therefore, this study is designed to investigate whether morphine dependence could modify structural plasticity of the hippocampal DG neurons and whether miR-132 is involved in mediating morphine dependence by regulating the structural plasticity. First, we established a morphine-dependent rat model and examined the structural plasticity of the DG. Second, μ-N2a cell line (N2a cells which stably express μ-opioid receptor) was used to demonstrate whether miR-132 mediated the morphine exposure-induced neuronal differentiation. Last, miR-132 sponge AAVs were injected into the DG of morphine-dependent rats to explore the effect of miR-132 on morphine dependence. This study will deepen our understanding towards the structural plasticity and transcriptional mechanism induced by morphine dependence.

2 | MATERIALS AND METHODS

2.1 | Morphine-dependent model

Adult male Sprague–Dawley rats weighing 250 g (8-week-old) were housed in a 12-h reverse light/dark cycle (lights on at 7:00 PM) environment. Rats were habituated for 1 week before experimentation. All the experimental procedures were performed in accordance with the National Institutes of Health Guide for the Care and Use of Laboratory Animals, and the procedures were approved by the Animal Use Committee of Peking University Health Science Center.

Morphine hydrochloride (First Pharmaceutical Factory of Qinghai, China) was dissolved in 0.9% saline to different concentrations. Rats in morphine-dependent group received intraperitoneal (i.p.) injection of morphine twice daily at 8:00 AM and 8:00 PM for 6 days with increasing doses (5, 10, 20, 40, and 80 mg/kg), and rats in saline group were intraperitoneal injected with equal volume of saline. Six hours after the last injection, all rats were intraperitoneal injected with 1 mg/kg naloxone (T0102, TargetMol, USA), and four different withdrawal signs (wet-dog shakes, teeth-chattering, diarrhoea, and ptosis) were observed for 30 min. Percentage of weight loss was calculated by difference of weight between the 30 min/weight before naloxone injection.

2.2 | Virus injection

Lentivirus encoding enhanced green fluorescent protein (EGFP) (GV248, GeneChem, Shanghai, China) or miR-132 sponge AAVs (Obio technology, Shanghai, China) were injected into the dorsal DG 3 and 7 days, respectively, before morphine injections. The injection sites were 3.6 and 6.0 mm posterior to the Bregma, 2.2 and 5.2 mm to the midline, and 3.8 mm ventral from the pia mater surface.

2.3 | Neuronal morphological analyses

Rats were sacrificed 6 h after the last morphine injection to avoid the effect of single morphine exposure. Morphological structure of the DG neurons was labelled by EGFP carried by lentivirus or AAVs. Sholl analyse was done as we described previously.[9] Secondary dendrites of the DG granular neurons under high magnification (100× objective) were taken for spine density calculation. The total spine amount and dendritic length were measured by ImageJ, and the spine density was calculated by the formula: (total spine amount/dendritic length) * 10.

2.4 | Establishment of μ-N2a cell line and drug treatment

N2a cells were stably transfected with MOR-1 overexpression vector pCMV6-Entry (OriGene) using transfection reagent Megatran 1.0 (OriGene) and subsequently selected by culturing in the presence of 1 mg/ml of G418. The selected clones were then maintained under a humidified atmosphere with 5% CO_2 in Dulbecco's modified Eagle's medium supplemented with 10% fetal bovine serum, 100 μg/ml streptomycin, 100 IU/ml penicillin, and 500 μg/ml of G418. In Figures 3D

and 4A,B, μ-N2a cells were treated with increasing doses of morphine hydrochloride. Cells were collected after 15-min or 24-h morphine treatment. In Figure 4D, μ-N2a cells were treated with 20-μM retinoic acid (R2625, Sigma-Aldrich, USA) and collected after 0, 24, 48, 72, and 96 h.

2.5 | Real-time qPCR

The qPCR was performed according to the protocols described previously.[9] The primer sequences were used in our published article[9] and shown in Table 1.

2.6 | Immunofluorescence

Cells were washed by PBS three times and incubated with 4% paraformaldehyde (PFA) for 30 min at room temperature to fix the cells and then washed by PBS three times. For brain slices, rats were perfused by 4% PFA and dehydrated for 7 days according to our previous paper. Then brains were quick-frozen in liquid nitrogen and were cut into coronal sections of 50 μm using freezing microtome. The stain protocol was described in our previous research.[10]

The primary antibodies were anti-MOR-1 (ab10275, Abcam, San Francisco, CA, USA) and anti-MAP 2 (4542, Cell Signaling Technology, Danvers, MA, USA). The secondary antibody was Alexa Fluor 555-conjugated donkey anti-rabbit IgG (A31572, Invitrogen, Carlsbad, CA, USA).

2.7 | Flow cytometry

Cells were collected and incubated in culture medium containing CD24 antibody (1:400, BD, Franklin Lake, NJ, USA) for 25 min at 4°C (protected from light) and were resuspended softly once in the middle of the incubation time. After washed by PBS with 5% fetal bovine serum (5% FBS), cells were resuspended in 1-ml 5% FBS and analysed on FCM Caliber (BD Biosciences, San Jose, CA, USA). Data were analysed by Flow Jo.

2.8 | Statistical analyses

Student's *t* tests were used for comparisons between two groups. One-way ANOVA was used for comparisons between three or more groups. Two-way ANOVA was used for comparisons with two factors. Chi-square test was used to compare parameters of incidence rate. Two-way repeated measures ANOVA was used in Sholl analysis.

3 | RESULTS

3.1 | Morphine dependence could induce the structural plasticity of granular cells in the DG

To mimic human opioid dependence, morphine-dependent rat model was established by repeated morphine administration.[26] Following the administration of increasing doses of morphine twice a day for six consecutive days, rats were given a single injection of naloxone (1 mg/kg, i.p.) at 6 h after the last morphine injection to avoid the acute effect of single morphine exposure. Naloxone-precipitated withdrawal symptoms were monitored for 30 min to verify whether the dependent model was successfully established (Figure 1A). More rats in the morphine group suffered from diarrhoea (Figure 1B, chi-square test, $z = 2.59$, $df = [6.667, 1]$, $^{**}p = 0.0098$) and ptosis (Figure 1C, chi-square test, $z = 2.59$, $df = [7.892, 1]$, $^{**}p = 0.005$) than in the saline group, and rats in the morphine group showed more wet dog shakes (Figure 1D, unpaired *t* test, 3.33 ± 0.96 vs. 18.70 ± 4.62, $df = 17$, $^{*}p = 0.0273$), teeth-chattering (Figure 1E, unpaired *t* test, 0.33 ± 0.17 vs. 6.2 ± 2.29, $df = 17$, $^{**}p = 0.0066$), and weight loss (Figure 1F, unpaired *t* test, 1.47 ± 0.21 vs. 3.27 ± 0.7, $df = 17$, $^{*}p = 0.0326$), implying that the rats in the morphine group successfully developed morphine dependence.

To label the granular cells in the DG, CMV-EGFP lentivirus was injected into the dorsal DG 3 days before morphine exposure, and the

TABLE 1 The primer sequences of GAPDH, miR-132, and miR-212

Gene	Primers	Sequence (5′ → 3′)
GAPDH	RT primer	TGGCAAAGTGGAGATTGTT
	Sense	CTTCTGGGTGGCAGTGAT
	Antisense	TGGCAAAGTGGAGATTGTT
miR-132	RT primer	GTCGTATCCAGTGCAGGGTCCGAGGTATTCGCACTGGATACGACCGACCAT
	Sense	CGCTAACAGTCTACAGCC
	Antisense	GCAGGGTCCGAGGTATTC
miR-212	RT primer	GTCGTATCCAGTGCAGGGTCCGAGGTATTCGCACTGGATACGACTGGCCGT
	Sense	ATCGCTAACAGTCTCCAGTC
	Antisense	GCAGGGTCCGAGGTATTC

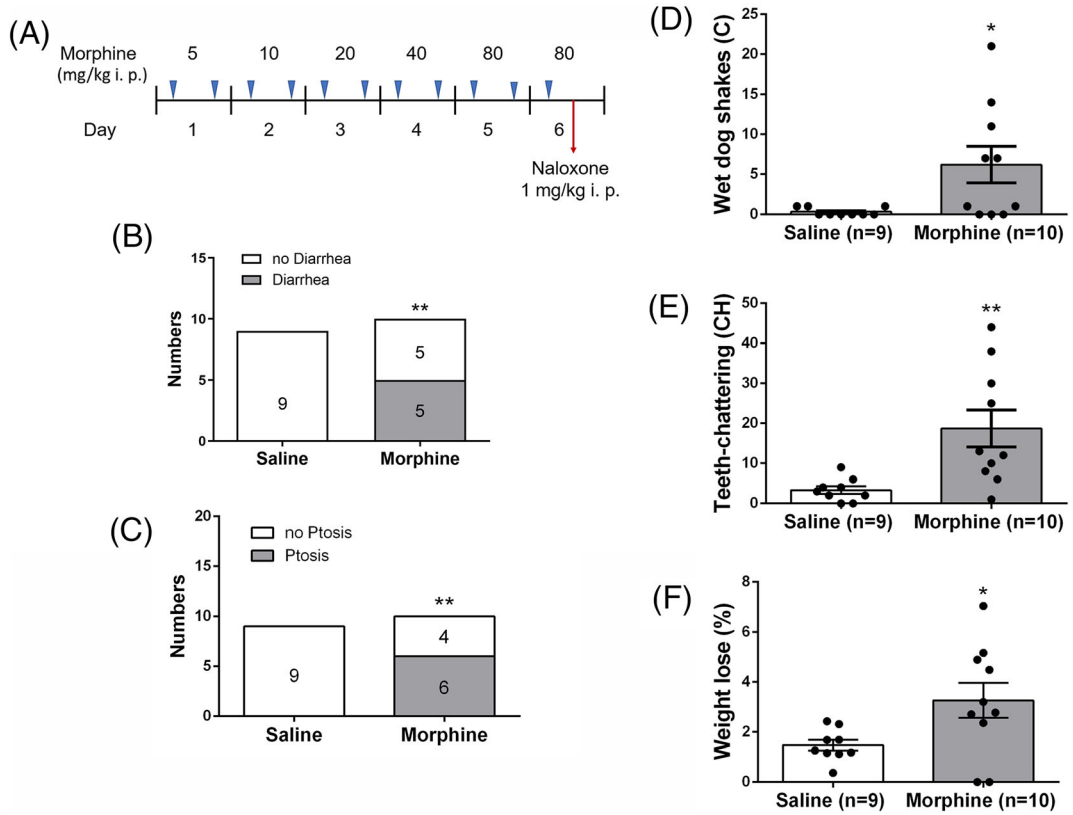

FIGURE 1 Increasing doses of morphine-treated rats suffer from severe withdrawal symptoms after naloxone-precipitated withdrawal. (A) Schematic of experimental procedures. Rats in morphine group show more diarrhoea (B), ptosis (C), wet dog shakes (D), teeth-chattering (E), and weight loss (F) than in saline groups; $^{**}p < 0.01$, chi-square test (B,C); $^{*}p < 0.05$, $^{**}p < 0.01$, unpaired Student's *t* test (E, F). Data are shown as mean ± SEM

brain was perfused and fixed 6 h after the last morphine injection (Figure 2A–D). Sholl analysis showed that the dendritic tree of granular cells in the DG of morphine-dependent rats was significantly more complex than that of control rats (Figure 2E, two-way repeated measures ANOVA, interaction: $F(29, 986) = 1.26$, $p > 0.05$; row factor: $F(29, 986) = 35.89$, $^{****}p < 0.0001$; column factor: $F(1, 34) = 7.18$, $^{*}p = 0.0113$), and the dendritic spine density was also increased in morphine dependent rats (Figure 2F, unpaired *t* test, 8.08 ± 0.61 vs. 13.47 ± 0.70, $df = 28$, $^{****}p < 0.0001$). These structural changes indicated that the formation of morphine dependence was coincident with the increase of branching and restructuring of the dendrite of DG neurons. Therefore, the adaptational restructuring of DG neurons may be a potential mechanism underlining formation of morphine dependence.

3.2 | miR-132 mediated longer term morphine treatment-induced μ-N2a cell differentiation

N2a cell line was used to investigate the effect of morphine on neuronal structural plasticity and its underlying molecular mechanism. Since N2a cells express nearly no mu-opioid receptor (MOR), we generated an N2a cell line stably expressing MOR-1 (μ-N2a). μ-N2a cells homogeneous expressed MOR-1 and could eliminate the faint effect of delta-opioid receptor (DOR) and kappa-opioid receptor (KOR), so μ-N2a cell line was an appropriate model for study of the MOR-mediated intracellular molecular mechanisms.[27] Briefly, N2a cells were transfected with MOR-1 overexpression vector containing neomycin resistance gene. When grown in medium containing G418 selection agent, the μ-N2a stable cell line was generated. MOR overexpression was verified by immunofluorescence (Figure 3A), qPCR for mRNA abundance (Figure 3B, unpaired *t* test, 1.000 ± 0.0 vs. 13,263 ± 2791, $df = 6$, $^{**}p = 0.0032$), and western blot (Figure 3C) for protein level.

To distinguish the impact of morphine treatment on the structural plasticity of μ-N2a cells, we added different concentrations of morphine (0, 10, 100, and 1000 μM) to the culture medium and collected the cells after 15 min and 24 h, respectively. Fixed cells were labelled by nuclear marker Hoechst 33258 and cytoskeleton marker MAP-2 (Figure 3D$_i$). The percentage of neurite^{+} cells and total dendritic length were increased after 24-h morphine treatment, but not 15-min morphine treatment, especially in the 100-μM and 1000-μM groups (Figure 3D$_{ii}$, two-way ANOVA with Tukey's multiple comparisons test, 24 h–Vehicle vs. 24 h–10 μM, $df = 24$, $^{***}p < 0.001$; 24 h–Vehicle vs. 24 h–100 μM, $df = 24$, $^{****}p < 0.0001$; 24 h–Vehicle

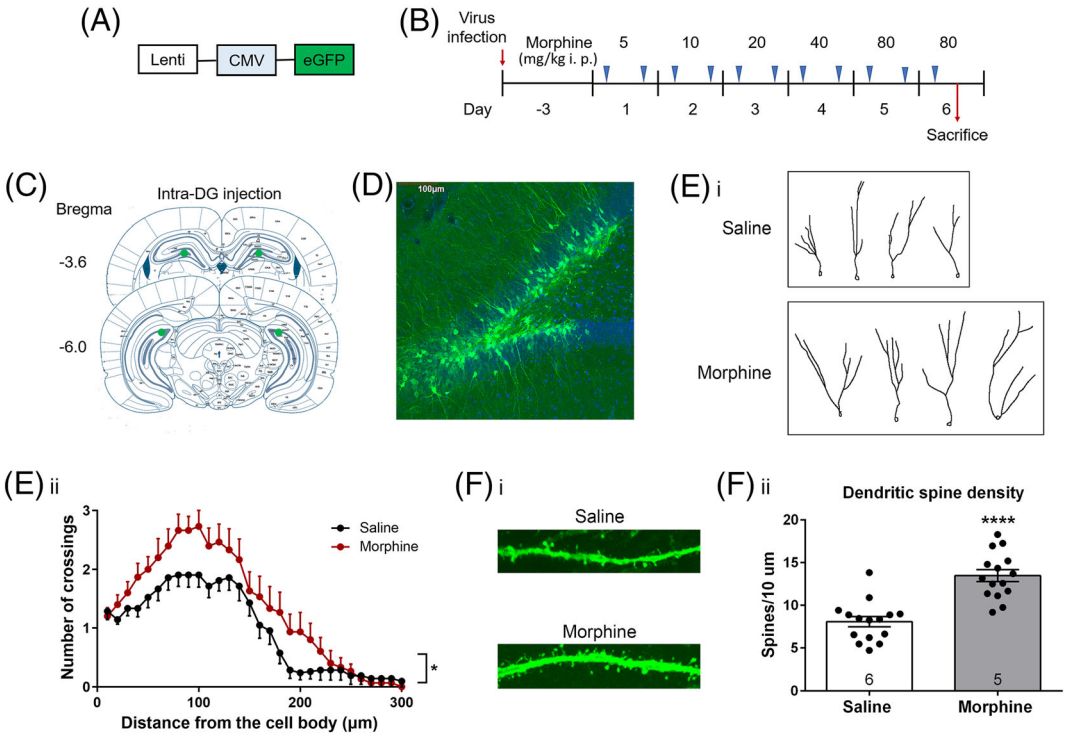

FIGURE 2 Morphine dependence increases the structural plasticity of the hippocampal DG neurons. (A) Structural diagram of the label virus. (B) Schematic of experimental procedures. (C) Injection sites in the dorsal DG. (D) Representative images of the labelled neurons; scale bar: 100 μm. (E) Morphine dependence increases the dendrite complexity of the DG neurons. (i) Representative structure diagrammatic sketches of dendritic trees of the DG neurons. (ii) Dendritic trees of the DG neurons in the morphine group are more complex than in the saline group; $^{*}p < 0.05$, two-way ANOVA repeated measures. (F) Morphine dependence increases the spine density of the DG neurons. (i) Representative diagrams of the dendrites of DG neurons after morphine dependence. (ii) The dendritic spine density of DG neurons is obviously increased after morphine dependence; $^{****}p < 0.0001$, unpaired Student's *t* test. Data are shown as mean ± SEM

vs. 24 h–1000 μM, $df = 24$, $^{****}p < 0.0001$) (Figure $3D_{iii}$, two-way ANOVA with Tukey's multiple comparisons test, 24 h–Vehicle vs. 24 h–100 μM, $df = 34$, $^{****}p < 0.0001$; 24 h–Vehicle vs. 24 h–1000 μM, $df = 34$, $^{****}p < 0.0001$). These results indicated that longer term and higher concentrations of morphine treatment could increase the neuronal differentiation and structural plasticity of μ-N2a cells.

Then we investigated the possible role of miR-132 in longer term morphine treatment-induced structural plasticity. We examined the expression of miR-132/212 after 15-min and 24-h morphine treatment. qPCR results showed that miR-132/212 expression was significantly increased after 1000-μM morphine treatment (24 h) (Figure 4A, two-way ANOVA with Tukey's multiple comparisons test, 24 h–Vehicle vs. 24 h–100 μM, $df = 32$, $^{*}p < 0.05$; 24 h–1000 μM, $df = 32$, $^{***}p < 0.001$) (Figure 4B, two-way ANOVA with Tukey's multiple comparisons test, 24 h–1000 μM, $df = 24$, $^{**}p < 0.01$). Additionally, correlating with the neuronal differentiation induced by 20-μM retinoic acid (RA) (Figure 4C), miR-132/212 expression was gradually increased in a time-dependent pattern (Figure $4D_i$ [left], one-way ANOVA, $F(4, 10) = 0.4951$, $^{**}p = 0.0094$, multiple comparisons: 0 h vs. 96 h, $^{*}p < 0.05$) (Figure $4D_i$ [right], one-way ANOVA, $F(4, 20) = 1.093$, $^{**}p = 0.0073$, multiple comparisons: 0 h vs. 96 h, $^{**}p < 0.01$). Since the increase of miR-132 expression was significantly higher than that of miR-212 (Figure $4D_{ii}$, two-way ANOVA with Tukey's multiple comparisons test, interaction: $F(4, 30) = 3.68$, $^{*}p < 0.05$; row factor: $F(4, 30) = 13.70$, $^{****}p < 0.0001$; column factor: $F(1, 30) = 13.32$, $^{**}p = 0.001$; multiple comparisons: miR-132–0 h vs. miR-132–96 h, $^{*}p < 0.05$; miR-212–0 h vs. miR-212–96 h, $^{**}p < 0.01$; miR-132–96 h vs. miR-212–96 h, $^{\#}p < 0.05$), we inferred that miR-132 was the main effector in neuronal differentiation. Next, we used flow cytometry to analyse the expression of neuronal differentiation marker CD24 on the membrane. Longer term morphine treatment significantly shifted the peak of CD24 expression histogram to the right (Figure $4E_i$), and the percentage of cells highly expressing CD24 was increased (Figure $4E_{ii}$, unpaired *t* test, vehicle vs. morphine, 60.28 ± 2.34 vs. 75.78 ± 3.39, $df = 6$, $^{**}p = 0.0094$). In addition, overexpression of miR-132 showed a similar effect with longer term morphine treatment, whereas miR-132 knockdown had no effect (Figure 4F, one-way ANOVA, $F(3, 15) = 1.715$, $^{****}p < 0.0001$; multiple comparisons: Ctrl vs. OE, $^{**}p < 0.01$; Scrm vs. OE, $^{**}p < 0.01$). We surmised that this was due to the low expression level of miR-132 in the untreated μ-N2a cells, so we transfected miR-132 knockdown plasmid before morphine treatment

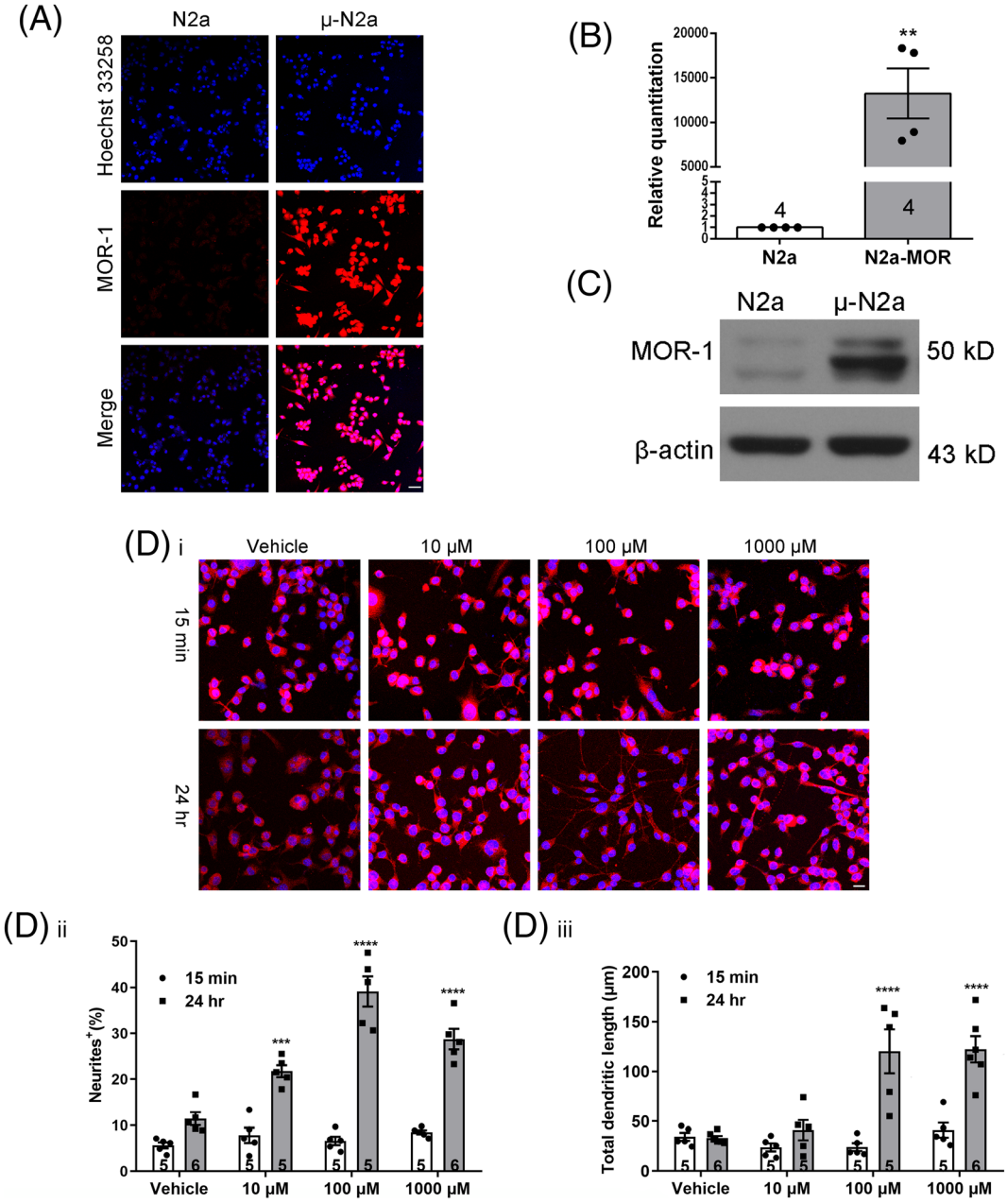

FIGURE 3 Longer term morphine treatment induces neuronal differentiation of μ-N2a cells. (A) Representative diagrams of N2a cells and stable MOR-overexpressed N2a cells; cells are labelled by nuclear marker Hoechst 33258 (blue) and MOR-1 (red), scale bar: 50 μm. (B) The expression of MOR mRNA is dramatically increased in μ-N2a cells; $^{**}p < 0.01$, unpaired Student's *t* test. (C) A representative western blot result showing MOR-1 protein level in N2a cells and μ-N2a cells. (D) Longer term morphine treatment advances differentiation of μ-N2a cells in a dose-dependent pattern. (i) Representative diagrams of μ-N2a cells after different concentrations of 15-min or 24-h morphine treatment; cells are labelled by nuclear marker Hoechst 33258 (blue) and cytoskeleton marker MAP-2 (red), scale bar: 20 μm. (ii) The percentage of neurites^{+} cells are increased after longer term morphine treatment; $^{***}p < 0.001$, $^{****}p < 0.0001$, compared with 24 h–vehicle group, two-way ANOVA with Tukey's multiple comparisons test. (iii) Longer term and higher concentrations of morphine treatment increase total neurite length of μ-N2a cells. $^{****}p < 0.0001$, compared with 24 h–vehicle group, two-way ANOVA with Tukey's multiple comparisons test. Data are shown as mean ± SEM

and found that miR-132 knockdown significantly reversed the neuronal differentiation (indicated by CD24 expression) induced by longer term morphine treatment (Figure 4G, unpaired *t* test, M + Scrm vs. M + KD, 49.89 ± 0.62 vs. 24.9 ± 6.10, $df = 12$, $^{**}p = 0.0016$). In conclusion, miR-132 was responsible for the longer term morphine treatment-induced structural plasticity in μ-N2a cells.

3.3 | Morphine dependence-induced neuronal structural plasticity of the DG was mediated by miR-132

In view of the consensus that repeated morphine treatment can lead to dependence and adaptive changes of dendritic structure by

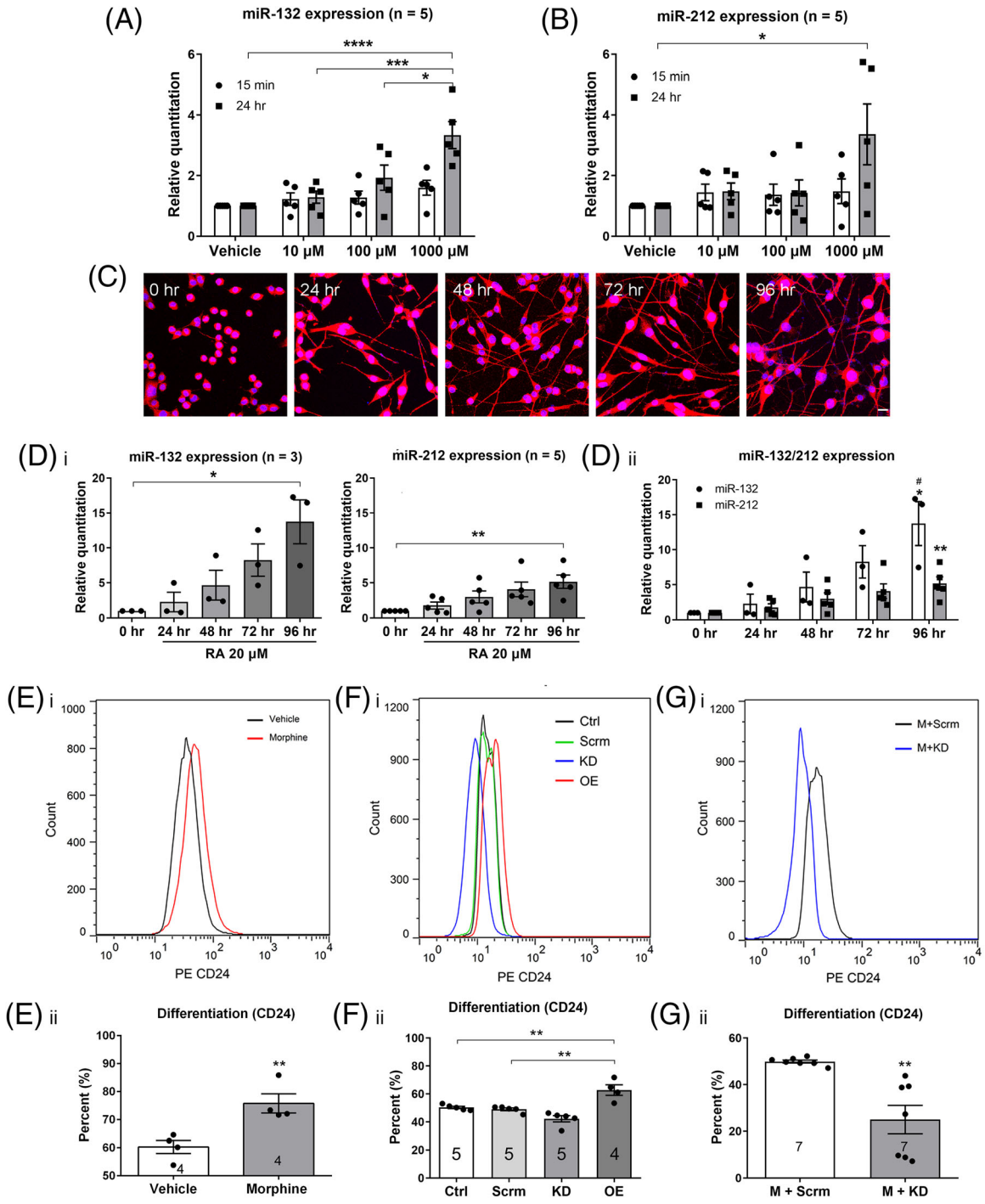

FIGURE 4 The expression of miR-132 can be induced by longer term morphine treatment and neuronal differentiation. (A, B) Longer term and higher doses of morphine treatment increase the expression of miR-132 and miR-212; $^{*}p < 0.05$, $^{**}p < 0.01$, $^{***}p < 0.001$, compared with 24 h–vehicle group, two-way ANOVA with Tukey's multiple comparisons test. (C) Representative diagrams of μ-N2a cells after RA treatment at different time points; cells are labelled by nuclear marker Hoechst 33258 (blue) and cytoskeleton marker MAP-2 (red), scale bar: 20 μm. (D) The expression of miR-132/212 is increased after RA treatment by a time-dependent pattern. (i) RA treatment increases miR-132/212 expression; $^{*}p < 0.05$, $^{**}p < 0.01$, one-way ANOVA with Tukey's multiple comparisons test. (ii) The increase in expression of miR-132 is more obviously than miR-212; $^{*}p < 0.05$, $^{**}p < 0.01$, compared with 0 h; $^{\#}p < 0.05$, compared with iR-212–96 h; two-way ANOVA with Tukey's multiple comparisons test. (E) Longer term morphine treatment accelerates the differentiation of μ-N2a cells. (i) A representative flow cytometry image of P-phycoerythrin (PE) CD24. (ii) Quantification of differentiation using fluorescence intensity; $^{**}p < 0.01$, unpaired Student's *t* test. (F) miR-132 overexpression accelerates the differentiation of μ-N2a cells. (i) A representative flow cytometry image of P-phycoerythrin (PE) CD24. (ii) Quantification of differentiation using fluorescence intensity; $^{**}p < 0.01$, one-way ANOVA. (G) miR-132 knockdown reverses the neuronal differentiation induced by longer term morphine treatment. (i) A representative flow cytometry image of P-phycoerythrin (PE) CD24. (ii) Quantification of differentiation using fluorescence intensity; $^{**}p < 0.01$, unpaired Student's *t* test. Data are shown as mean ± SEM

activating CREB signalling in rodents,[3] we speculated that CREB-regulated miRNA, miR-132, may involve in morphine dependence. Thus, we examined the expression of miR-132/212 at the same time-point with the structural analysis (Figure 5A) and found that dorsal DG of the rats in the morphine group expressed significantly more miR-132/212 than in the saline group (Figure 5B, unpaired *t* test, saline vs. morphine, 1.02 ± 0.02 vs. 6.78 ± 2.17, $df = 6$, $^{*}p = 0.038$) (Figure 5C, unpaired *t* test, saline vs. morphine, 1.11 ± 0.07 vs. 4.477 ± 1.399, $df = 8$, $^{*}p = 0.0133$), indicating that the expression of miR-132 was elevated during the formation of morphine dependence.

Mature miR-132 has two forms, miR-132 3p and miR-132 5p, which are cleaved by Dicer from the pre-miRNA-132 and mediate different physiological functions (Figure 6A). Therefore, two different sponge sequences against miR-132 3p and miR-132 5p, respectively, were designed, and CaMKII promoter was used in AAVs to specifically express the sponges in the excitatory neurons (Figure 6B–D). Structural analysis showed that morphine dependence increased the complexity of dendritic trees and the spine density of DG neurons, and these effects could be reversed by miR-132 3p sponge, but not miR-132 5p sponge (Figure 6E,F) (Figure $6E_{ii}$, saline–control vs. morphine–control: two-way repeated measures ANOVA, interaction: $F(29, 406) = 0.72$, $p = 0.8625$; row factor: $F(29, 406) = 27$, $^{***}p < 0.000167$; column factor: $F(1, 14) = 26.5$, $^{***}p = 0.0001 < 0.000167$; multiple comparisons row 13: saline + control vs. morphine + control, $^{*}p < 0.05$) (Figure $6E_{ii}$, morphine + control vs. morphine + 3p sponge: two-way repeated measures ANOVA, interaction: $F(29, 406) = 1.033$, $p = 0.4215$; row factor: $F(29, 406) = 30.3$, $^{***}p < 0.000167$; column factor: $F(1, 14) = 10.2$, $^{*}p = 0.0065 < 0.0083$; multiple comparisons row 22: morphine + control vs. morphine + 3p sponge, $^{\#}p < 0.05$) (Figure $6F_{ii}$, two-way ANOVA with Tukey's multiple comparisons test, interaction: $F(2, 27) = 3.423$, $^{*}p = 0.0433$; row factor: $F(1, 37) = 23.55$, $^{****}p < 0.0001$; column factor: $F(2, 27) = 5.81$, $^{**}p = 0.0064$; multiple comparisons: saline + control vs. morphine + control, $df = 37$, $^{**}p < 0.01$; saline + 5p sponge vs. morphine + 5p sponge, $df = 37$, $^{*}p < 0.05$; morphine + control vs. morphine + 3p sponge, $df = 37$, $^{\#\#}p < 0.01$), indicating that the structural plasticity induced by morphine dependence was mediated by miR-132 3p.

Last, miR-132 sponge AAVs were transfected into the dorsal DG before morphine injection and naloxone-precipitated withdrawal symptoms were monitored in rats (Figure 7A). miR-132 3p sponge, but not 5p sponge, largely reduced the percentage of morphine-dependent rats that suffered from diarrhoea (Figure 7B, saline–control vs. morphine–control: chi-square test, $z = 3.795$, $df = (14.4, 1)$, $^{***}p = 0.0001 < 0.000167$; saline–5p sponge vs. morphine–5p sponge: chi-square test, $z = 3.513$, $df = (12.34, 1)$, $^{**}p = 0.0004 < 0.00167$) and ptosis (Figure 7C, saline–control vs. morphine–control: chi-square test, $z = 3.795$, $df = (14.4, 1)$, $^{***}p = 0.0001 < 0.000167$; saline–5p sponge vs. morphine–5p sponge: chi-square test, $z = 3.513$, $df = (12.34, 1)$, $^{**}p = 0.0004 < 0.00167$). Meanwhile, rats in the morphine–3p sponge group also showed significantly less teeth-chattering (Figure 7D, two-way ANOVA with Tukey's multiple comparisons test, interaction: $F(2, 43) = 3.763$, $p = 0.0312$; row factor: $F(1, 43) = 45.11$, $^{****}p < 0.0001$; column factor: $F(2, 43) = 3.111$, $p = 0.0547$; multiple comparisons: saline–control vs. morphine–control, $^{****}p < 0.0001$, saline–5p sponge vs. morphine–5p sponge, $^{***}p < 0.001$, saline–3p sponge vs. morphine–3p sponge, $p > 0.05$, morphine–control vs. morphine–3p sponge, $^{\#}p < 0.05$) and wet dog shakes (Figure 7E, two-way ANOVA with Tukey's multiple comparisons test, interaction: $F(2, 43) = 2.027$, $p = 0.1441$; row factor: $F(1, 43) = 17.84$, $^{***}p = 0.0001$; column factor: $F(2, 43) = 2.129$, $p = 0.1314$; multiple comparisons: saline–control vs. morphine–control, $^{*}p < 0.05$, saline–5p sponge vs. morphine–5p sponge, $^{*}p < 0.05$) than those in the morphine–control group without changes in weight loss (Figure 7F, two-way ANOVA with Tukey's multiple comparisons test, interaction: $F(2, 43) = 0.06416$, $p = 0.9379$; row factor: $F(1, 43) = 32.13$, $^{****}p < 0.0001$; column factor: $F(2, 43) = 0.1041$, $p = 0.9014$; multiple comparisons: saline–control vs. morphine–control, $^{*}p < 0.05$, saline–5p sponge vs. morphine–5p sponge, $^{*}p < 0.05$). These results showed that inhibiting the function of miR-132 3p but not 5p, could disturb the formation of morphine dependence. Taken together, miR-132 3p but not 5p in the DG neurons mediated morphine dependence.

4 | DISCUSSION

In this work, we found that miR-132 could mediate neuronal differentiation induced by 24-h morphine exposure in vitro. In vivo, morphine dependence was associated with increased neuronal structural

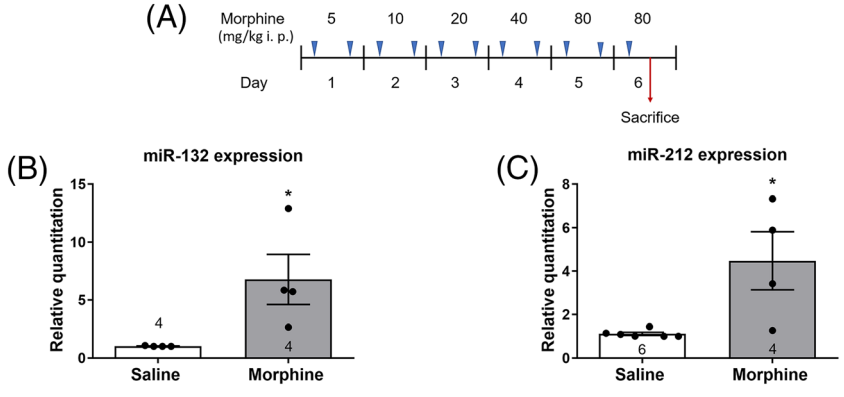

FIGURE 5 The expression of miR-132/212 is increased in the hippocampal DG after morphine dependence. (A) Schematic of experimental procedures. (B) The expression of miR-132 is increased after morphine dependence; $^{*}p < 0.05$, unpaired Student's *t* test. (C) The expression of miR-212 is increased after morphine dependence; $^{*}p < 0.05$, unpaired Student's *t* test. Data are shown as mean ± SEM

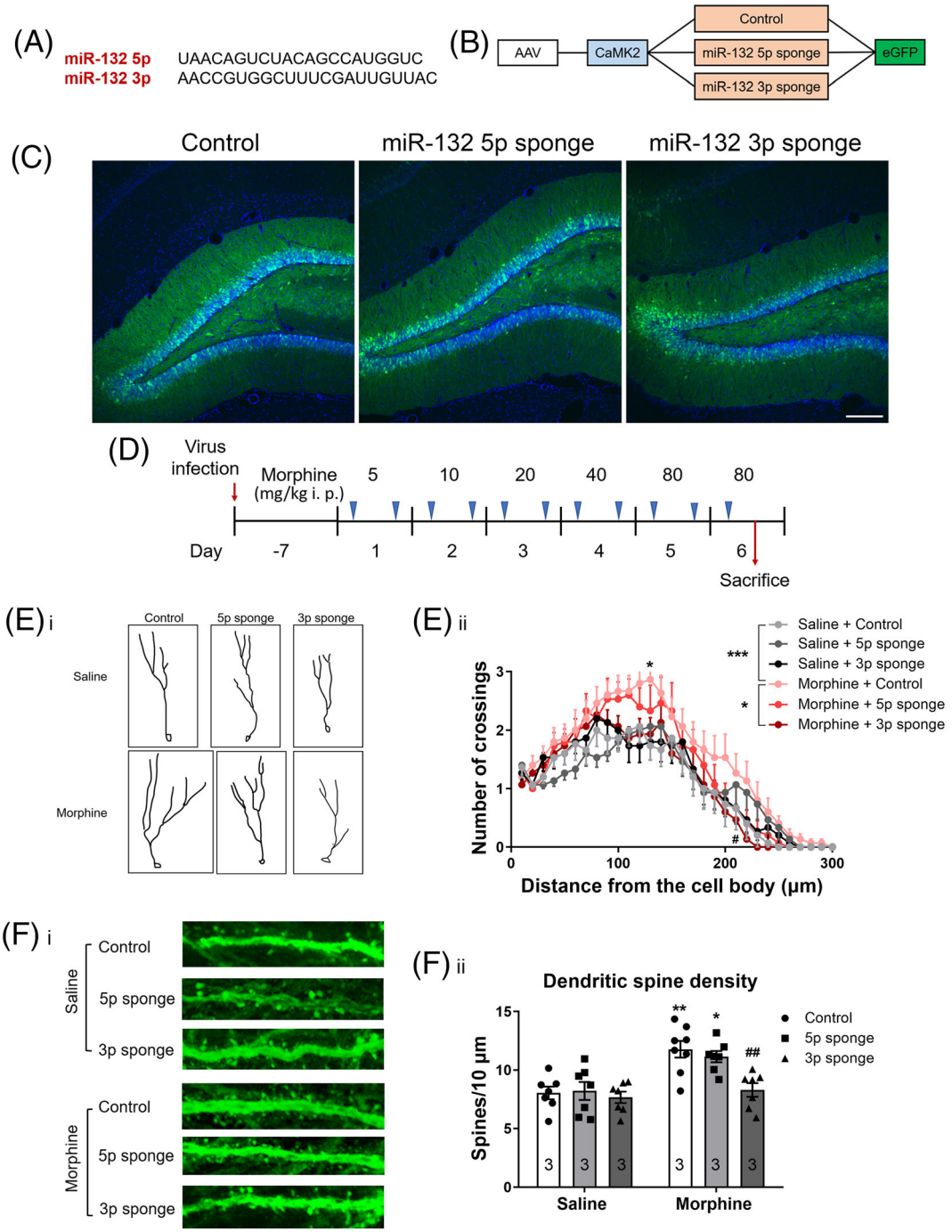

FIGURE 6 miR-132 3p but not 5p inhibition reverses the structural plasticity of the hippocampal DG neurons induced by morphine dependence. (A) The nucleotide sequence of miR-132 3p/5p. (B) Structural diagram of the miR-132 sponge virus. (C) Representative images of the hippocampal DG 7 days after virus transfection, scale bar: 100 μm. (D) Schematic of experimental procedures. (E) miR-132 3p but not 5p inhibition reverses the dendrite complexity increase induced by morphine dependence. (i) Representative structure diagrammatic sketches of dendritic trees of the DG neurons. (ii) The dendrite complexity of the DG neurons is increased after morphine dependence, which can be reversed by miR-132 3p sponge; $^{*}p < 0.05$, $^{**}p < 0.01$, two-way ANOVA repeated measures with multiple adjustment. (F) miR-132 3p but not 5p inhibition reverses the spine density increase induced by morphine dependence. (i) Representative diagrams of the dendrites of DG neurons. (ii) The spine density of the DG neurons is increased after morphine dependence, which can be reversed by miR-132 3p sponge; $^{*}p < 0.05$, $^{**}p < 0.01$, compared with saline group; $^{\#}p < 0.05$, compared with morphine–control group; two-way ANOVA with Tukey's multiple comparisons test. Data are shown as mean ± SEM

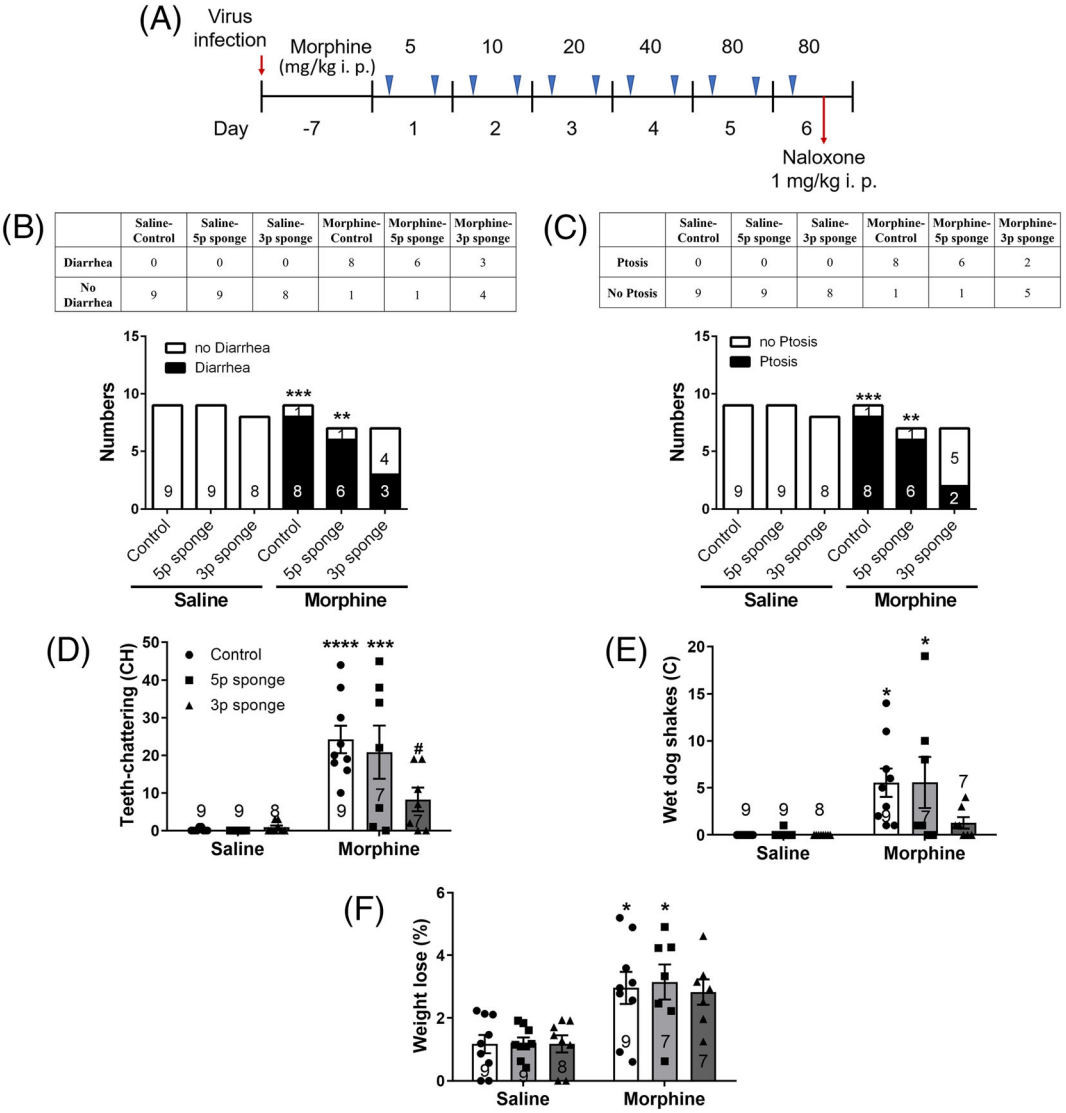

	Saline-Control	Saline-5p sponge	Saline-3p sponge	Morphine-Control	Morphine-5p sponge	Morphine-3p sponge
Diarrhea	0	0	0	8	6	3
No Diarrhea	9	9	8	1	1	4

	Saline-Control	Saline-5p sponge	Saline-3p sponge	Morphine-Control	Morphine-5p sponge	Morphine-3p sponge
Ptosis	0	0	0	8	6	2
No Ptosis	9	9	8	1	1	5

FIGURE 7 miR-132 3p but not 5p inhibition relieves morphine withdrawal symptoms. (A) Schematic of experimental procedures. (B, C) Significantly more control rats and miR-132 5p sponge rats but not miR-132 3p sponge rats in morphine group show diarrhoea or ptosis than in saline group; $^{**}p < 0.01$, compared with saline, two-way ANOVA with Tukey's multiple comparisons test. (D, E) Number of wet dog shakes and teeth-chattering are increased in morphine group, which can be decreased by miR-132 3p sponge; $^{****}p < 0.0001$, compared with saline; $^{\#}p < 0.05$, compared with morphine–control group; two-way ANOVA with Tukey's multiple comparisons test. (F) Rats in morphine group lose more weight than in saline group; $^{****}p < 0.0001$, two-way ANOVA with Tukey's multiple comparisons test. Data are shown as mean ± SEM

plasticity and miR-132 expression in the DG of rats. Introduction of miR-132 3p sponge rather than miR-132 5p sponge into the DG not only reversed the morphine-dependent structural plasticity but also inhibited morphine withdrawal symptoms in rats. These findings indicate that miR-132 3p is one of the important molecules that mediate morphine dependence.

4.1 | Morphine-induced neuronal structural plasticity and morphine dependence

In 1999, Robinson and Kolb first reported that chronic morphine treatment significantly decreased the branches and spine density of dendritic trees of medium spiny neurons (MSNs) in the nucleus accumbens (NAc).[28] Since then, numerous studies aimed on the structural plasticity of neurons induced by addictive drugs and found that opiates decreased the dendritic complexity and spine density of NAc MSNs, mPFC and hippocampus pyramidal neurons, but stimulants such as cocaine played the opposite role.[21,28] However, our results demonstrated that 24-h morphine treatment in vitro could increase the percentage of neurites^{+} cells and the total dendritic length of μ-N2a cells, and morphine dependence also increased the dendrite complexity and spine density of hippocampal DG granular neurons. Actually, recent research also showed that the effect of morphine on structural plasticity of neurons was not unidirectional. For example, Kobrin et al. reported that morphine CPP could increase the total

dendritic length and branch number of MSNs in the NAc core, while passively receiving the same dose of morphine increased the dendritic spine density,[29] indicating that different administration protocols may lead to distinct results. Additionally, we think three other factors could also have influenced morphine-induced structural plasticity. First, different animal models and administration paradigms: most previous studies administered morphine in equal dose during the entire procedure, mainly reflecting morphine tolerance, but we treated rats with increasing doses of morphine, simulating the formation process of morphine dependence in physiological state. Second, different sacrifice time points: previous studies always collected the brain tissue during withdrawal period or after CPP test, which would be deeply affected by the serious withdrawal symptoms and the CPP test. In this work, we collected the brain tissue at 6 h after the last morphine injection to avoid the acute effect of single morphine exposure (the half-life of morphine is 2–4 h) and the effect of long-term abstinence (>24 h)-induced emotional and mental symptoms. Third, our work focused on the hippocampal DG, which is not one of the traditional members of the reward system like LC, NAc, VTA, PFC, and hippocampal CA1,[1,21,30] but increasing evidence has shown that the DG is not only involved in morphine-associated memory but also in morphine dependence.[11–15]

4.2 | miR-132 was involved in mediating neuronal structural plasticity

We have demonstrated in this work that in vitro expression of miR-132 was coincident with differentiation of μ-N2a cells and miR-132 overexpression significantly promoted differentiation of μ-N2a while miR-132 knockdown showed the opposite effect. In vivo, we found that inhibiting miR-132 3p in the rats' DG reversed the morphine dependence-induced dendritic morphogenesis and spinogenesis, implying that miR-132 might participate in morphine dependence by modulating the neuronal structural plasticity of the rats' DG.

The structural plasticity of spines includes changes in density and morphology. miR-132 has been shown to modify the structural plasticity of spines by regulating different target genes. On one hand, miR-132 overexpression in the forebrain may significantly increase spine density of the CA1 pyramidal neurons by down-regulating the expression of MeCP2.[25] On the other hand, miR-132 overexpression in the hippocampal neurons increased the spine area, head area, head length and head width of the mushroom spines without altering spine density, and such effects were mediated by MMP-9 down-regulation by miR-132.[31] In a word, miR-132 can precisely regulate the density and morphology of spines on the hippocampal neurons via different target genes. In our study, multiple structural changes occurred in the DG when miR-132 was inhibited, including morphological change of the dendritic trees and change of spine density. Thus, miR-132 may mediate morphine dependence-induced structural plasticity by regulating multiple target genes. Further studies are needed to elucidate how miR-132 regulates the plasticity of the DG neurons in morphine-dependent rats and the exact target genes mediating different morphological changes.

4.3 | miR-132, one of the transcriptional mechanisms involved in morphine dependence

Morphine dependence can lead to numerous abnormal behaviours that can be generally divided into two types: physical dependence behaviours including wet dog shakes, diarrhoea, teeth-chattering, ptosis, weight loss, and so on, and psychological responses including craving for re-use of drug and compulsive drug seeking behaviour. These physical and psychological responses have been documented to associate with a lot of gene expression, so the most investigated mechanism of morphine dependence is the transcriptional mechanism.[32] Morphine binds to opioid receptors on neurons that belong to G-coupled receptors, which can activate downstream second massagers such as cAMP, and induce the phosphorylation of CREB by protein kinase A. CREB, which acts as a transcription factor, can regulate expression of numerous addiction-related genes including miR-132. Moreover, CREB and ΔFosB are the firstly identified transcriptional factors involved in morphine dependence.[32]

Besides transcriptional factors, miRNAs also participate in mediating morphine dependence. In our research, morphine treatment in μ-N2a cells and rats could induce the expression of miR-132. Jimenez-Gonzalez et al. also reported that morphine exposure (48 h) significantly increased the expression of miR-132 and BDNF in zebrafish embryos, and miR-132 knockdown blocked morphine-induced BDNF expression. This effect may be mediated by relieving the inhibition on BDNF expression by MeCP2, which is suppressed by miR-132.[33] These studies indicate that morphine is involved in modifying neuronal differentiation by regulating the expression of miR-132–MeCP2–BDNF signalling and are partly confirmed by our results that miR-132 inhibition reversed neuronal differentiation of granular neurons in the DG and relieved withdrawal syndromes induced by morphine dependence (Figures 6 and 7).

4.4 | The functional difference between miR-132 3p and 5p

According to our work, inhibition of miR-132 3p but not miR-132 5p could significantly relieve morphine dependence-induced withdrawal syndromes and structural plasticity modulation of DG neurons, indicating that miR-132 3p and 5p have different functions. miR-132 3p and 5p are partially complementary mature miRNA-132 that are cleaved by RNase III enzyme, Dicer-1, from the 3′ and 5′ residue respectively of precursor miRNA-132.[34] Since miR-132 5p has relatively poor stability and can be easily degraded by Dicer, it was traditionally named miR-132* and its function was poorly understood.[35–38] Magill et al. reported that the activity of miR-132 3p gradually increased along with the differentiation of hippocampal neurons in vitro and in vivo with no change in miR-132 5p,[39] indicating that miR-132 3p but not 5p mediates neuronal differentiation.

In conclusion, our study reveals that miR-132 3p but not 5p is involved in morphine dependence via modifying the structural plasticity of the DG neurons in rats. Further studies are needed to

investigate the downstream signalling of miR-132 that mediates the structural plasticity and morphine dependence.

ACKNOWLEDGMENTS

We thank for grants from the National Basic Research Development Program of China (2015CB553500), the National Natural Science Foundation of China (81471353 and 81771433), the Natural Science Foundation of Beijing (7214224).

CONFLICT OF INTERESTS

The authors declare no competing interests.

AUTHORS CONTRIBUTION

Meng Jia, Xuewei Wang, and Cailian Cui conceived the study. Xuewei Wang, Meng Jia, and Haolin Zhang performed the experiments on μ-N2a cells in vitro. Meng Jia, Xinjuan Wang, Hui Ma, and Mingda Yang performed the experiments on rats in vivo. Meng Jia analysed the data and wrote the original draft. Cailian Cui and Yijing Li reviewed and edited the manuscript.

DATA AVAILABILITY STATEMENT

The data that support the findings of this study are available from the corresponding author upon reasonable request.

ORCID

Cailian Cui https://orcid.org/0000-0002-8638-8258

REFERENCES

1. Eric N. Under siege: the brain on opiates. *Neuron*. 1996;16(5):897-900.
2. Strang J, Volkow ND, Degenhardt L, et al. Opioid use disorder. *Nat Rev Dis Primers*. 2020;6(3):1-28.
3. Nestler EJ. Molecular neurobiology of addiction. *Am J Addict*. 2001;10(3):201-217.
4. Robinson TE, Kolb B. Structural plasticity associated with exposure to drugs of abuse. *Neuropharmacology*. 2004;47(Suppl 1):33-46.
5. Sklair-Tavron L, Shi WX, Lane SB, Harris HW, Bunney BS, Nestler EJ. Chronic morphine induces visible changes in the morphology of mesolimbic dopamine neurons. *Proc Natl Acad Sci U S A*. 1996;93(20):11202-11207.
6. Robinson TE, Kolb B. Persistent structural modifications in nucleus accumbens and prefrontal cortex neurons produced by previous experience with amphetamine. *J Neurosci*. 1997;17(21):8491-8497.
7. Van Dijk MT, Fenton AA. On how the dentate gyrus contributes to memory discrimination. *Neuron*. 2018;98(4):832-845.
8. Ge F, Wang N, Cui C, et al. Glutamatergic projections from the entorhinal cortex to dorsal dentate gyrus mediate context-induced reinstatement of heroin seeking. *Neuropsychopharmacology*. 2017;42(9):1860-1870.
9. Jia M, Wang X, Zhang H, et al. MicroRNA-132 in the adult dentate gyrus is involved in opioid addiction via modifying the differentiation of neural stem cells. *Neurosci Bull*. 2019;35(3):486-496.
10. Zhang H, Jia M, Wang XW, et al. Dentate gyrus μ-opioid receptor-mediated neurogenic processes are associated with alterations in morphine self-administration. *Sci Rep*. 2019;9(1471):1-11.
11. Martínez-aorden E, Navarro-aragoza J, Milanés M, Laorden M, Almela P. Conditioned aversive memory associated with morphine withdrawal increases brain-derived neurotrophic factor in dentate gyrus and basolateral amygdala. *Addict Biol*. 2020;25(4):1-11, e12792.
12. Valero E, Gómez-Milanés I, Almela P, et al. The involvement of CRF1 receptor within the basolateral amygdala and dentate gyrus in the naloxone-induced conditioned place aversion in morphine-dependent mice. *Prog Neuropsychopharmacol Biol Psychiatry*. 2018;84(Pt a):102-114.
13. Wan L, Su L, Xie Y, Liu Y, Wang Z. Protein receptor for activated C kinase 1 is involved in morphine reward in mice. *Neuroscience*. 2009;161(3):734-742.
14. Lowe AS, Williams SCR, Symms MR, Stolerman IP, Shoaib M. Functional magnetic resonance neuroimaging of drug dependence: naloxone-precipitated morphine withdrawal. *Neuroimage*. 2002;17(2):902-910.
15. Erdtmann-Vourliotis M, Mayer P, Riechert U, Grecksch G, Höllt V. Identification of brain regions that are markedly activated by morphine in tolerant but not in naive rats. *Brain Res Mol Brain Res*. 1998;61(1–2):51-61.
16. Nestler EJ. A general role for adaptations in G-proteins and the cyclic AMP system in mediating the chronic actions of morphine and cocaine on neuronal function. *Brain Res*. 1645;2016:71-74.
17. Nestler EJ. Transcriptional mechanisms of addiction: role of DeltaFosB. *Philos Trans R Soc Lond B Biol*. 2008;363(1507):3245-3255.
18. Nestler EJ. Is there a common molecular pathway for addiction? *Nat Neurosci*. 2005;8(11):1445-1449.
19. Nestler EJ. Molecular mechanisms of drug addiction. *Neuropharmacology*. 2004;47(7):24-32.
20. Dietz DM, Dietz KC, Nestler EJ, Russo SJ. Molecular mechanisms of psychostimulant-induced structural plasticity. *Pharmacopsychiatry*. 2009;42(S 01):S69-S78.
21. Russo SJ, Dietz DM, Dumitriu D, Morrison JH, Malenka RC, Nestler EJ. The addicted synapse: mechanisms of synaptic and structural plasticity in nucleus accumbens. *Trends Neurosci*. 2010;33(6):267-276.
22. Nudelman AS, Dirocco DP, Lambert TJ, et al. Neuronal activity rapidly induces transcription of the CREB-regulated microRNA-132, in vivo. *Hippocampus*. 2010;20(4):492-498.
23. Qian Y, Song J, Ouyang Y, et al. Advances in roles of miR-132 in the nervous system. *Front Pharmacol*. 2017;8(770):1-9.
24. Wayman GA, Monika D, Hideaki A, et al. An activity-regulated microRNA controls dendritic plasticity by down-regulating p250GAP. *Proc Natl Acad Sci U S a*. 2008;105(26):9093-9098.
25. Hansen KF, Kensuke S, Wayman GA, Soren I, Karl O. Transgenic miR132 alters neuronal spine density and impairs novel object recognition memory. *Plos One*. 2010;5(11):1-7, e15497.
26. Li YJ, Zhong F, Yu P, Han JS, Wu LZ. Electroacupuncture treatment normalized sleep disturbance in morphine withdrawal rats. *Evid Based Complement Alternat Med*. 2011;2011(5):1-8, 361054.
27. Chakrabarti S, Law PY, Loh HH. Neuroblastoma Neuro2A cells stably expressing a cloned μ-opioid receptor: a specific cellular model to study acute and chronic effects of morphine. *Brain Res Mol Brain Res*. 1995;30(2):269-278.
28. Robinson TE, Kolb B. Morphine alters the structure of neurons in the nucleus accumbens and neocortex of rats. *Synapse*. 2015;33(2):160-162.
29. Kobrin KL, Moody O, Arena DT, Moore CF, Heinrichs SC, Kaplan GB. Acquisition of morphine conditioned place preference increases the dendritic complexity of nucleus accumbens core neurons. *Addict Biol*. 2016;21(6):1086-1096.
30. Williams JT, Christie MDJ, Manzoni OJ. Cellular and synaptic adaptations mediating opioid dependence. *Physiol Rev*. 2001;81(1):299-343.
31. Jasińska M, Miłek J, Cymerman IA, Łęski S, Kaczmarek L, Dziembowska M. miR-132 regulates dendritic spine structure by

direct targeting of matrix metalloproteinase 9 mRNA. *Mol Neurobiol*. 2016;53(7):4701-4712.
32. Nestler EJ, Hope BT, Widnell KL. Drug addiction: a model for the molecular basis of neural plasticity. *Neuron*. 1993;11(6):995-1006.
33. Jimenez-Gonzalez A, García-Concejo A, López-Benito S, Gonzalez-Nunez V, Arévalo JC, Rodriguez RE. Role of morphine, miR-212/132 and mu opioid receptor in the regulation of Bdnf in zebrafish embryos. *Biochim Biophys Acta*. 2016;1860(6):1308-1316.
34. Fukunaga R, Han BW, Hung JH, Xu J, Weng Z, Zamore PD. Dicer partner proteins tune the length of mature miRNAs in flies and mammals. *Cell*. 2012;151(3):533-546.
35. Meng Y, Shao C, Gou L, Chen YJ. Ming. Construction of MicroRNA- and MicroRNA*-mediated regulatory networks in plants. *RNA Biol*. 2011;8(6):1124-1148.
36. Yang HF, Zheng WH, Zhao WT, Guan CY, An J. Roles of miR-590-5p and miR-590-3p in the development of hepatocellular carcinoma. *Nan Fang Yi Ke Da Xue Xue Bao*. 2013;33(6):804-811.
37. Griffiths-Jones S, Grocock RJ, van Dongen S, Bateman A, Enright AJ. miRBase: microRNA sequences, targets and gene nomenclature. *Nucleic Acids Res*. 2006;34(Database issue):140-144.
38. Yonemori M, Seki N, Matsushita R, et al. Dual tumor-suppressors miR-139-5p and miR-139-3p targeting matrix metalloprotease 11 in bladder cancer. *Cancer Sci*. 2016;107(9):1233-1242.
39. Magill ST, Cambronne XA, Luikart BW, et al. microRNA-132 regulates dendritic growth and arborization of newborn neurons in the adult hippocampus. *Proc Natl Acad Sci U S A*. 2010;107(47):20382-20387.

How to cite this article: Jia M, Wang X, Zhang H, et al. MicroRNA-132 is involved in morphine dependence via modifying the structural plasticity of the dentate gyrus neurons in rats. *Addiction Biology*. 2022;27(1):e13086. doi:10.1111/adb.13086